3D In Vitro Ultrasound Super-Resolution Imaging using a Clinical System

Kirsten Christensen-Jeffries
Department of Biomedical Engineering, King's College London
London, UK
kirsten.christensen-jeffries@kcl.ac.uk

Jemma Brown
Department of Biomedical Engineering, King's College London
London, UK
jemma.brown@kcl.ac.uk

Sevan Harput
Department of Bioengineering, Imperial College London
London, UK
s.harput@imperial.ac.uk

Ge Zhang
Department of Bioengineering, Imperial College London
London, UK
ge.zhang15@imperial.ac.uk

Jiaqi Zhu
Department of Bioengineering, Imperial College London
London, UK
j.zhu16@imperial.ac.uk

Meng-Xing Tang[†]
Department of Bioengineering, Imperial College London
London, UK
mengxing.tang@imperial.ac.uk

Christopher Dunsby[†]
Department of Physics, Imperial College London
London, UK
christopher.dunsby@imperial.ac.uk

Robert Eckersley[†]
Department of Biomedical Engineering, King's College London
London, UK
robert.eckersley@kcl.ac.uk

[†] These authors contributed equally to this work.

***Abstract*—Assessment of complex and disordered tumour vasculature requires full 3D visualization. Ultrasound super-resolution techniques are able to image microvascular structure and flow beyond the diffraction limit. Existing demonstrations have been predominantly 2D, where the elevational resolution remains restricted to around the millimeter range, while 3D demonstrations have either used mechanical scanning, or have required customized or state-of-the-art research systems to achieve true super-resolution in the third dimension. In this study, 3D super-resolution and velocity tracking is demonstrated *in vitro* using an ultrasound imaging system currently available in the clinic. This was performed at 1.25 MHz transmit frequency, with a frame rate of 54 Hz in contrast enhanced imaging mode. Three-dimensional super-resolved volumetric imaging of a twisted micro-vessel phantom was demonstrated at 3.5 cm depth, where between 66-70% of localizations where estimated to fall within the vessel internal diameter. Demonstration of 3D ultrasound super-resolution using a system currently available in the clinic demonstrates a fast route for clinical translation and application. In the future, 3D localization using microbubble signal onset could allow considerably improved microvascular visualization to aid early disease detection, diagnosis, and intervention for micro-vascular related diseases like cancer.**

Keywords — ultrasound, super-resolution, microbubbles, contrast, 3d imaging.

I. Introduction

The structure and flow of the microcirculation reflects the requirements and conditions of local cells and tissue. Thus, visualizing the presence, structure and function of blood vessels is crucial for clinical assessment. Architectural changes in the micro-vascular structure, as well as variations in vascular flow can be a marker of pathological, damaged or dysfunctional tissue, such as ischemia [1], and peripheral arterial disease (PAD) [2]–[5], while an increase can indicate rapid and uncontrollable cell growth or proliferation caused by cancer and metastasis [6]–[9]. Detecting such microscopic changes *in vivo* using non-invasive high-resolution imaging would allow early clinical intervention and would provide a means of closely monitoring the treatment of such diseases.

Recently developed ultrasound super-resolution (US-SR) imaging has been able to generate spatially resolved maps of fine micro-vessels *in vitro* and *in vivo* by imaging the isolated signals from microbubble contrast agents [10]–[18]. These techniques have been demonstrated using both clinical US systems with only video data access [10]–[12], [17] and research systems with RF data access [13]–[16], [18], with the latter techniques often making use of high frame-rate plane wave imaging [19]–[22].

Assessment of complex and disordered tumour vasculature requires full 3D visualization. Much of this previous work has been based around the use of 1-D linear array transducers that has restricted the super-resolved image information to 2D [10]–[12], [17], [18]. Here, as well as in the case of 3-D volume acquisition using mechanical scanning in the third dimension [13], [15], [23], the elevational resolution remains a limiting factor. Ultrasound super-resolution techniques require an acquisition strategy which can additionally localize bubbles in the elevational plane with high precision to enable full 3D assessment. Demonstrations of super-resolution in all three dimensions have included the use of a hemi-spherical sparse array through an *ex vivo* skull phantom [13], the use of a bespoke matrix array transducer to image a tilted phantom structure [14], and orthogonal compounding with two synchronized linear array transducers [16].

As yet, the benefits of RF data processing for localisation precision have not been fully investigated, and ultrasound super-resolution methods have been able to demonstrate significant improvements in spatial resolution even with the restricted data accessibility provided by unmodified clinical US systems operating in a standard B-mode or contrast enhanced mode [10]–[12], [17]. A number of image based-post-processing methods have been developed [11], [12], [24], where localisation precisions under 10 μm have been demonstrated.

Existing demonstrations of super-resolution have been predominantly 2D, where the elevational resolution remains restricted to around the millimeter range, while 3D

demonstrations have required customized or state-of-the-art research systems to achieve true super-resolution in the third dimension. In this study, 3D super-resolution and velocity tracking is demonstrated *in vitro* using an ultrasound imaging system currently available in the clinic providing access to only beamformed and enveloped volumetric video data.

II. Materials and Methods

A. Ultrasound Equipment and Acquisition

Data were acquired using a clinical Philips EPIQ7 system with a X5-1 2D matrix array transducer. This 3040 element probe has a physical size of 2.9 x 3.9 x 9.2 cm and was used to transmit ultrasound waves at 1.25 MHz frequency in contrast enhanced imaging mode.

B. Phantom Generation

Phantoms were developed for 3D US imaging using medium density paraffin gel wax [25] and thin walled cellulose capillary tubes (Hemophan®, Membrana) of internal diameter 200 µm ± 15 µm (specifications provided by the manufacturer) (Figure 1A). These phantoms allow repeated use and optical validation due to transparency of material. To create the phantom, firstly, paraffin gel wax was placed into a silicone mold using sterile gloves in a clean environment to limit the possibility of small fragments and dust particles embedding in the phantom. This was heated to 105°C in an electric laboratory oven for approximately 2 hours. A coiled cellulose tube with inner diameter of 200 µm was embedded into the paraffin approximately 10 minutes after removing the phantom from the oven. This was then trimmed and inserted into 25G butterfly winged infusion needles at either end. An epoxy resin was used to secure the connections between the tubes and the needles. The speed of sound within the phantom was estimated to be 1425 ± 3 m/s using a reflection substitution technique.

C. In Vitro Microbubble Imaging

An infusion pump was used to circulate a dilution of SonoVue (Bracco, Milan) microbubbles (100 µl SonoVue™ in 600 ml water) through the phantom, which provided a suitable concentration for imaging spatially isolated microbubble signals. Imaging was performed at 54 volumes per second at a depth of 3.5 cm. Video segments were acquired for 11 seconds each. A rolling background subtraction was applied to remove unwanted background signals. Bubbles were then localized by calculating the onset of the extracted signal, as described in [24], adapted to 3D where the microbubble localization x and z-coordinate, x_l and z_l, were provided by the lateral and elevational intensity weighted center of mass. Twenty-three segments were processed in the final images. Microbubble tracking algorithms developed in our previous work [11] were extended for 3D implementation to determine the flow velocity within the micro-vessel structure. A tube centerline was estimated by finding the average axial and elevational position of the localizations across the lateral direction. The absolute distance of each localization to the nearest point in the tube centerline was calculated to assess the performance of the technique.

D. Image Generation

A 3D rendering of the combined localizations was constructed by plotting each estimated bubble location, r_l =

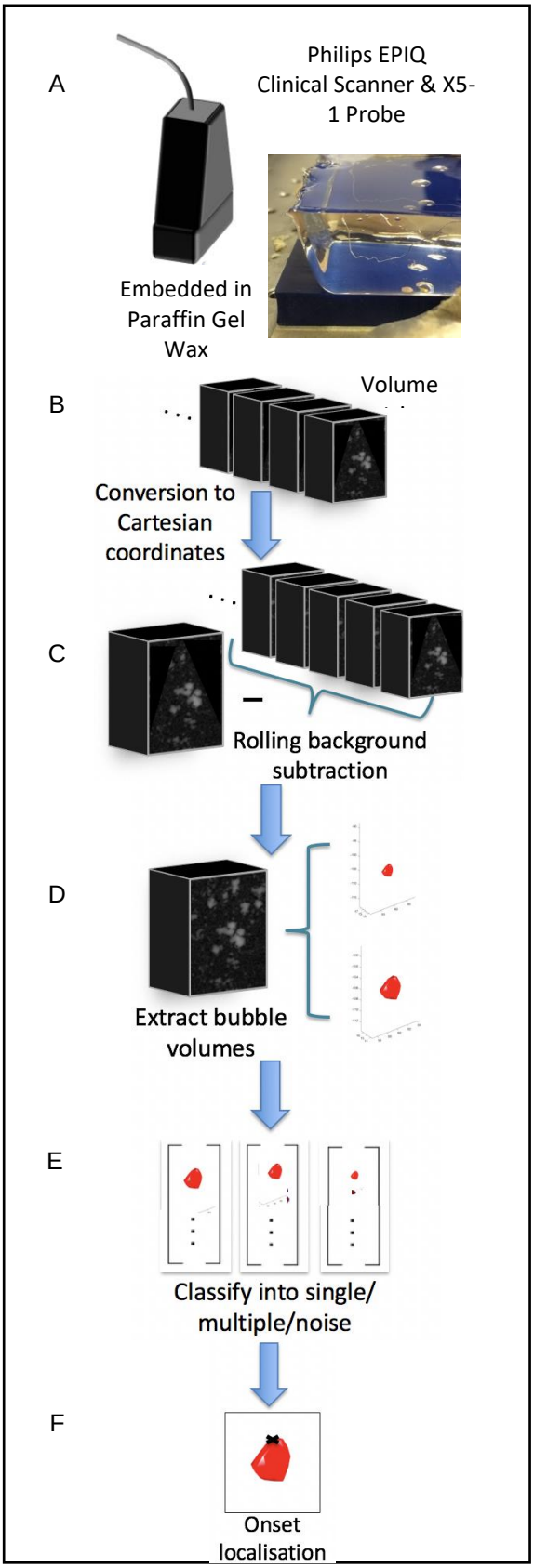

Figure 1. Ultrasound super-resolution method. (A) Volumetric ultrasound acquisition was performed using contrast enhanced ultrasound imaging on a twisted micro-vessel tube embedded within a gel phantom. Data were converted to cartesian coordinates, (B), before a rolling background subtraction was applied, (C), to extract bubble volumes (D). Those classified as single bubbles, (E), were localized (F). These localizations were combined to create the final super-resolution rendering.

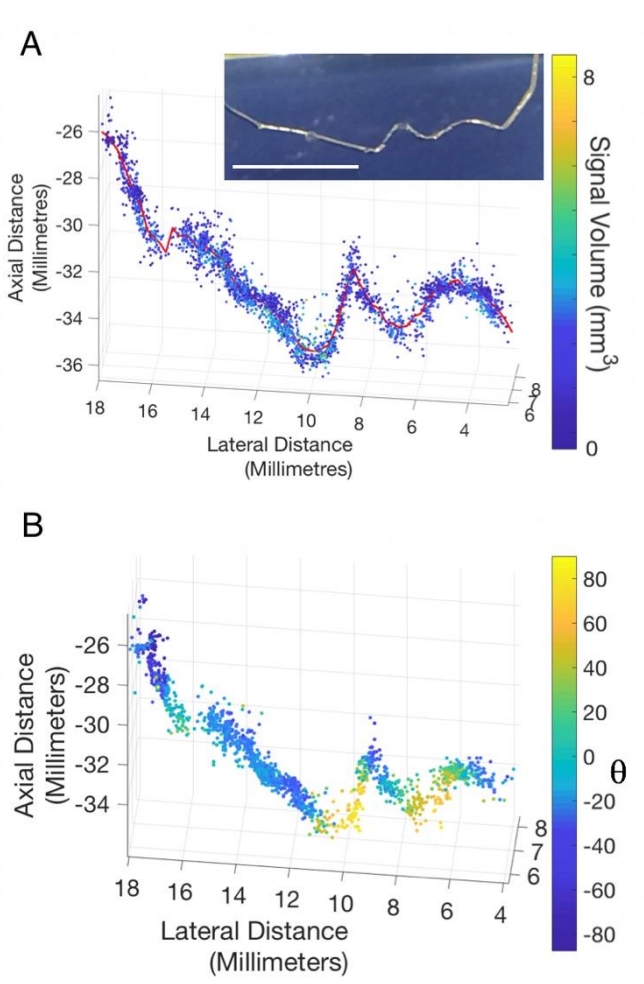

Figure 2. (A) A diffraction limited CEUS volume with a high microbubble concentration. (B) Three-dimensional localisation map of twisted tube using onset method with centreline in red. Optical image of phantom inset, scale bar 5 mm. (C) Three dimensional onset localizations with color bar representing elevational angle, θ.

(x_l, y_l, z_l), as an ellipsoid with semi-axis lengths equal to the previously estimated localization precisions in the axial, lateral and elevational directions, $\sigma = \sigma_x, \sigma_y, \sigma_z$, given by

$$\frac{(x - x_l)^2}{\sigma_x^2} + \frac{(y - y_l)^2}{\sigma_y^2} + \frac{(z - z_l)^2}{\sigma_z^2} = 1, \qquad (1)$$

where x, y, and z are the coordinates of any points on the surface of the ellipsoid. Microbubble tracking algorithms developed in our previous work [11] were extended for 3D implementation to determine the flow velocity within the micro-vessel structure. Intensity cross-correlations between each bubble signal in frame n and each of the bubble signals found in frame $n-1$ were then calculated and the maximum cross correlation was found for each signal in frame n. A pair of signals were considered to come from the same bubble if the maximum cross-correlation exceeded an empirically determined threshold of 0.7.

III. Results and Discussion

A diffraction limited CEUS volume with a high microbubble concentration is shown in Figure 2A. Three-dimensional super-resolved volumetric imaging of the twisted micro-vessel phantom was demonstrated with a clinical ultrasound system at depth (Figure 2B) providing improved visualization of the fine tubes. An optical image of the phantom structure is shown in the inset. Velocity tracking detected the direction of 3D velocity vectors as bubbles travel along the twisted structure (Figure 2C), where θ indicates the elevational angle of the velocity vector.

Absolute distances of onset localizations from the centerline are shown in Figure 3A. Corresponding histograms demonstrate 66% of the onset bubble localizations were inside the nominal internal diameter of the tube in a dry state (Figure D), up to a potential 70% if including a potential 15 µm error as specified by the manufacturer. With a specified possible length change of 8% in water, this percentage could potentially be even higher.

IV. Conclusion

In summary, this study demonstrates 3D ultrasound super-resolution is achievable using equipment currently available in the clinic by localizing the signals received from individual bubble signals within volumetric video data. Furthermore, this clinical acquisition strategy enables tracking of the bubbles in 3D to obtain 3D flow velocity information. The imaging frequency used in this study (1.25 MHz) indicates that this technique can be used for deep-tissue imaging. Additionally, the processing of enveloped data

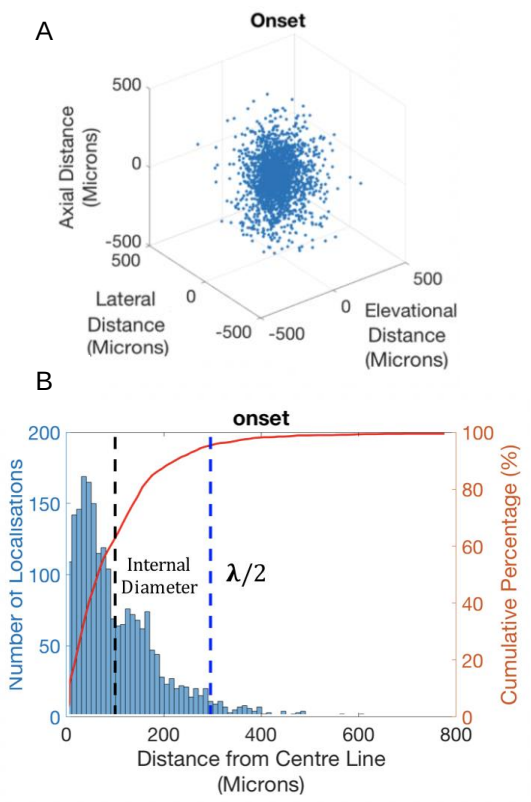

Figure 3. (A) The absolute distance of each localization from the nearest point in the centerline in all three dimensions. (B) Corresponding histogram of absolute distances from the centerline, where 66% of localizations are within the estimated internal diameter of the tube.

demonstrates that super-resolution is still possible without the large data sizes associated with raw RF data.

Demonstration of 3D ultrasound super-resolution using a system currently available in the clinic demonstrates a fast route for clinical translation and application. In the future, 3D localization using microbubble signal onset could allow considerably improved microvascular visualization to aid early disease detection, diagnosis, and intervention for micro-vascular related diseases like cancer.

ACKNOWLEDGMENT

This research was supported by the Department of Health via the National Institute for Health Research (NIHR) comprehensive Biomedical Research Center award to Guy's and St Thomas' NHS Foundation Trust in partnership with King's College London and King's College Hospital NHS Foundation Trust. The Centre of Excellence in Medical Engineering funded by the Wellcome Trust and EPSRC under grant number WT 088641/Z/09/Z. Additional funding provided by the EPSRC to King's College London and Imperial College London under grant numbers EP/N14855/1 and EP/N015487/1 respectively. The views expressed are those of the author(s) and not necessarily those of the NHS, the NIHR or the Department of Health.

REFERENCES

[1] K. Tuma, Ronald F. , Duran, Walter N. , Ley, *Microcirculation*. Academic Press, 2011.

[2] American Diabetes Association, "Peripheral Arterial Disease in People with Diabetes," *Diabetes Care*, vol. 26, no. 12, pp. 3333–3341, 2003.

[3] N. C. Dolan, K. Liu, M. H. Criqui, P. Greenland, J. M. Guralnik, C. Chan, J. R. Schneider, A. L. Mandapat, G. Martin, and M. M. McDermott, "Peripheral artery disease, diabetes, and reduced lower extremity functioning.," *Diabetes Care*, vol. 25, no. 1, pp. 113–20, Jan. 2002.

[4] R. Zatz and B. M. Brenner, "Pathogenesis of diabetic microangiopathy. The hemodynamic view," *Am. J. Med.*, vol. 80, no. 3, pp. 443–453, Mar. 1986.

[5] M. J. Fowler, "Microvascular and Macrovascular Complications of Diabetes," *Clin. Diabetes*, vol. 26, no. 2, pp. 77–82, Apr. 2008.

[6] N. Weidner, J. Folkman, F. Pozza, P. Bevilacqua, E. N. Allred, D. H. Moore, S. Meli, and G. Gasparini, "Tumor angiogenesis: a new significant and independent prognostic indicator in early-stage breast carcinoma.," *J. Natl. Cancer Inst.*, vol. 84, no. 24, pp. 1875–87, Dec. 1992.

[7] D. M. McDonald and P. L. Choyke, "Imaging of angiogenesis: from microscope to clinic.," *Nat. Med.*, vol. 9, no. 6, pp. 713–25, Jun. 2003.

[8] N. Weidner, "Intratumor microvessel density as a prognostic factor in cancer.," *Am. J. Pathol.*, vol. 147, no. 1, pp. 9–19, Jul. 1995.

[9] N. Weidner, J. P. Semple, W. R. Welch, and J. Folkman, "Tumor angiogenesis and metastasis--correlation in invasive breast carcinoma.," *N. Engl. J. Med.*, vol. 324, no. 1, pp. 1–8, Jan. 1991.

[10] O. M. Viessmann, R. J. Eckersley, K. Christensen-Jeffries, M. X. Tang, and C. Dunsby, "Acoustic super-resolution with ultrasound and microbubbles.," *Phys. Med. Biol.*, vol. 58, no. 18, pp. 6447–58, Sep. 2013.

[11] K. Christensen-Jeffries, R. J. Browning, M.-X. Tang, C. Dunsby, and R. J. Eckersley, "In Vivo Acoustic Super-Resolution and Super-Resolved Velocity Mapping Using Microbubbles," *IEEE Trans. Med. Imaging*, 2015.

[12] D. Ackermann, G. Schmitz, and S. Member, "Detection and Tracking of Multiple Microbubbles in Ultrasound B-Mode Images," vol. 63, no. 1, pp. 72–82, 2016.

[13] M. a O'Reilly and K. Hynynen, "A super-resolution ultrasound method for brain vascular mapping.," *Med. Phys.*, vol. 40, no. 11, p. 110701, Nov. 2013.

[14] Y. Desailly, O. Couture, M. Fink, and M. Tanter, "Sono-activated ultrasound localization microscopy," *Appl. Phys. Lett.*, vol. 103, no. 17, 2013.

[15] C. Errico, J. Pierre, S. Pezet, Y. Desailly, Z. Lenkei, O. Couture, and M. Tanter, "Ultrafast ultrasound localization microscopy for deep super-resolution vascular imaging," *Nature*, vol. 527, no. 7579, pp. 499–502, Nov. 2015.

[16] K. Christensen-Jeffries, J. Brown, P. Aljabar, M. Tang, C. Dunsby, and R. J. Eckersley, "3-D In Vitro Acoustic Super-Resolution and Super-Resolved Velocity Mapping Using Microbubbles," *IEEE Trans. Ultrason. Ferroelectr. Freq. Control*, vol. 64, no. 10, pp. 1478–1486, Oct. 2017.

[17] S. Harput, K. Christensen-Jeffries, J. Brown, Y. Li, K. J. Williams, A. H. Davies, R. J. Eckersley, C. Dunsby, and M.-X. Tang, "Two-Stage Motion Correction for Super-Resolution Ultrasound Imaging in Human Lower Limb," *IEEE Trans. Ultrason. Ferroelectr. Freq. Control*, vol. 65, no. 5, pp. 803–814, May 2018.

[18] P. Song, J. D. Trzasko, A. Manduca, R. Huang, R. Kadirvel, D. F. Kallmes, and S. Chen, "Improved Super-Resolution Ultrasound Microvessel Imaging With Spatiotemporal Nonlocal Means Filtering and Bipartite Graph-Based Microbubble Tracking," *IEEE Trans. Ultrason. Ferroelectr. Freq. Control*, vol. 65, no. 2, pp. 149–167, Feb. 2018.

[19] M. Tanter, J. Bercoff, L. Sandrin, and M. Fink, "Ultrafast compound imaging for 2-D motion vector estimation: application to transient elastography," *IEEE Trans. Ultrason. Ferroelectr. Freq. Control*, vol. 49, no. 10, pp. 1363–1374, Oct. 2002.

[20] G. Montaldo, M. Tanter, J. Bercoff, N. Benech, and M. Fink, "Coherent plane-wave compounding for very high frame rate ultrasonography and transient elastography," *IEEE Trans. Ultrason. Ferroelectr. Freq. Control*, 2009.

[21] M. Tanter and M. Fink, "Ultrafast imaging in biomedical ultrasound," *IEEE Trans. Ultrason. Ferroelectr. Freq. Control*, vol. 61, no. 1, pp. 102–119, Jan. 2014.

[22] O. Couture, S. Bannouf, G. Montaldo, J.-F. Aubry, M. Fink, and M. Tanter, "Ultrafast Imaging of Ultrasound Contrast Agents," *Ultrasound Med. Biol.*, vol. 35, no. 11, pp. 1908–1916, Nov. 2009.

[23] F. Lin, S. E. Shelton, D. Espíndola, J. D. Rojas, G. Pinton, and P. A. Dayton, "3-D Ultrasound Localization Microscopy for Identifying Microvascular Morphology Features of Tumor Angiogenesis at a Resolution Beyond the Diffraction Limit of Conventional Ultrasound," *Theranostics*, vol. 7, no. 1, pp. 196–204, 2017.

[24] K. Christensen-Jeffries, S. Harput, J. Brown, P. N. T. Wells, P. Aljabar, C. Dunsby, M.-X. Tang, and R. J. Eckersley, "Microbubble Axial Localization Errors in Ultrasound Super-Resolution Imaging," *IEEE Trans. Ultrason. Ferroelectr. Freq. Control*, vol. 64, no. 11, pp. 1644–1654, Nov. 2017.

[25] S. L. Vieira, T. Z. Pavan, J. E. Junior, and A. a O. Carneiro, "Paraffin-Gel Tissue-Mimicking Material for Ultrasound-Guided Needle Biopsy Phantom," *Ultrasound Med. Biol.*, vol. 39, no. 12, pp. 2477–2484, 2013.